A Piezoelectric Stick-slip Manipulator for a Holonomic Precision Mobile Robot

Ryosuke Kinoshita[1], Eiji Kusui[1], Hazumu Kusama[1], Yohei Tsukui[1], Rintaro Minegishi[1], Yuna Sugiyama[1], Yuta Sunohara[1], Chihiro Sekine[1], and Ohmi Fuchiwaki[1#]

1 Department of Mechanical Engineering, Yokohama National University, 79-1 Tokiwadai Hodogaya-ku, Yokohama, Kanagawa, Japan,
#Corresponding Author / Email: ohmif@ynu.ac.jp, TEL: +81-45-339-3693

KEYWORDS: Piezoelectric actuator, Stick-slip actuator, Mobile robot, Walking robot

In this study, we developed a piezoelectric stick-slip actuator for developing compact and precise manipulator for a holonomic precision mobile robot. Firstly, we have designed an actuator using the piezoelectric stick-slip phenomenon. Then, we defined a mechanical model of the actuator as two mass system, for analyzing the dynamic characteristics. In experiments, we measured the displacement of the actuator under several conditions. The maximum speed of Z-axis was 8.9 [mm/s], and the payload was 30 [g]. We also developed the compact manipulator with weight of 55.3 [g] and size of 47 [mm]×62 [mm]×48 [mm]. The manipulator has two degrees of freedom and consists of a Z-axis stage and tweezers for realizing compact and precise mobile manipulator.

NOMENCLATURE

m_m: Mass of a mechanism with a piezoelectric actuator (PA)
m_s: Mass of a slider
k_m: Stiffness of a mechanism with PA
c_m: Damping coefficient of the mechanism with PA
d: Enforced displacement of PA
l: Distance between a leverage and a pivot points of PA
L: Distance between the leverage and a pivot points of a rod
α: Displacement expansion ratio of the leverage; $\alpha=L/l$
x_s: Displacement of the slider
x_{s0}: Initial position of the slider during its stick motion
x_r: Displacement of the rod
x_m: Displacement of PA
F_N: Normal force to the slider
F_f: Friction force acted on the slider
μ_0: Coefficient of a static friction for F_f
μ_k: Coefficient of a kinetic friction for F_f
F_g: Gravity force acted on the slider
A_r: Designed amplitude displacement of the rod
A_{re}: Experimental value of A_r under quasistatic condition
T: Period of the stick motion
$\tilde{v}_s$: Approximated constant velocity of the slider
$\tilde{x}_s$: Approximated displacement of the slider

1. Introduction

In recent years, compact electronic devices, such as smart phones, wearable devices, micro electromechanical systems (MEMS) etc. have been developed remarkably. Additionally, electronic components inside them have been required to be more compact, achieve higher performance [1,2]. Based on such a social background, precision technologies of handling micro-objects have become more important. Micromanipulation technologies have been researched actively [3,4]. However, the precision positioning devices, in currently used, needs excessive sizes, weights, relative to the target objects. It caused some problems in terms of space, energy efficiency, and versatility.

One solution to solve this problem, we have studied small, lightweight, self-propelled robots for manipulation [5,6], and various studies have been conducted in the past [7,8]. In particular, robots driven by piezoelectric actuators have been studied widely because of their small size, light weight, and high resolution. [9,10,11]. In this laboratory, three degrees of freedom (3DoF) precision self-propelled mechanisms driven by piezoelectric actuators capable of holonomic motion has been developed, however a flexible small manipulator for this mechanism has not been developed yet. Therefore, the main purpose of this study is to develop the manipulator. As specific target values, the weight and size of the manipulation mechanism are set to be less than 100 [g] and less than 80 [mm]×80 [mm]×80 [mm] respectively, which are more compact than the self-propelled mechanism.

2. Holonomic self-propelled mechanism

Fig. 1 shows the configuration of the holonomic precision self-propelled mechanism, and table 1 shows its specification. It consists of two Y-shaped electromagnetic legs (EM1, EM2), 6 piezoelectric actuators (PAs), and parallel springs. Each PA is named PA_F, PA_B, PA_{R1}, PA_{L1}, and PA_{L2}. PAs are attached to each side of legs by parallel spring. Two legs have combined each other by PAs via parallel springs

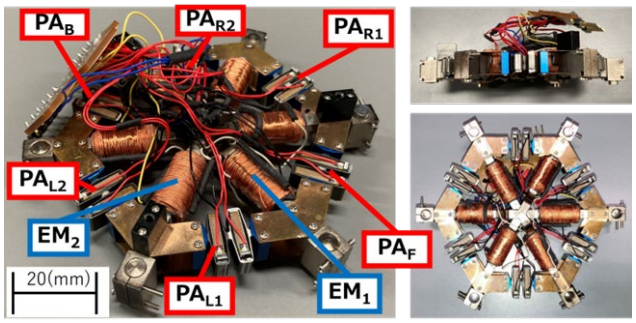

Fig. 1 The holonomic self-propelled mechanism

Table 1 Specification of the mechanism

Dimensions [mm]	86×86×11
Weight [g]	110
Maximum speed [mm/s]	10
Number of PA	6
Degree of freedom (DoF)	3 (X, Y, θ)

In walking, one leg is fixed to the ferromagnetic surface plate magnetically, and the other leg moves by the expansion and contraction of the 6 PAs. Repeating these motions, the mechanism can walk continuously. The mechanism has three degrees of freedom (3DoF) in XYθ axes; it can move translation, rotation, and revolution around any point, by appropriately adjusting the amount of expansion and contraction of each PAs. In other words, that realized holonomic movement.

3. Piezoelectric stick-slip actuator

3.1 Design

PA was chosen as the driving actuator for the manipulator. The actuator consists of a PA, a rod, and a linear slider, is driven using the stick-slip phenomenon caused by alternating slow and rapid deformations of PA. This phenomenon is caused by applying a sawtooth wave voltage to the PA. When the voltage changes slowly, the slider is moved on a stick motion, caused by static friction between the rod and slider, and the slider moves in accordance with the motion of the rod. On the other hand, when the changes rapidly, the static friction force is replaced to a kinetic friction, resulting in a slip motion. Due to the difference in inertia between the slider and the rod, only the rod moves during the slip motion, while the slider remains in place. The repetition of this motion, the slider can move continuously. In addition, applying an inverse sawtooth wave voltage enables the slider moving to an opposite direction. In result, the actuator can move bi-directional with only one PA.

The prototype actuator is shown Figure 2. The actuator was designed to be mounted on the self-propelled mechanism. It consists of a PA that is attached to the aluminum alloy rod frame, and a linear slider. To improve friction between the slider and the rod, an ABS friction chip is bonded to the tip of the rod, and a friction plate made from a ceramic sheet attached to the surface of the slider. In addition, a compression spring is inserted between the rod and the frame to apply a preload and increase the friction force between the rod and the slider.

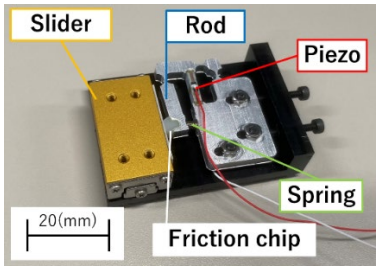

Fig. 2 The prototype actuator

3.2 Mechanical model

To analyze the dynamic characteristics of the actuator, we defined its mechanical model. It is expressed as two mass system of the actuator and slider as shown in Fig. 3.

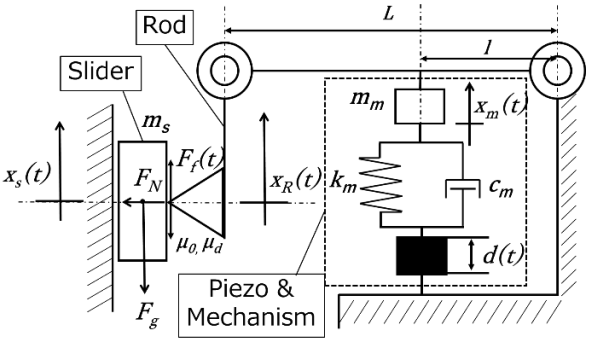

Fig. 3 Mechanical model

The equation of motion (EM) for the actuator is represented as,

$$m_m\ddot{x_m} + c_m(\dot{x_m} - \dot{d}) + k_m(x_m - d) = -F_f \quad (1)$$

Displacement of the rod x_r is approximately represented as the magnification of that of the actuator as below,

$$x_r = \alpha x_m \quad (2)$$

$$\alpha = \frac{L}{l} \quad (3)$$

From substituting (2) and (3) to (1), EM of the actuator using rod displacement x_R is represented as below,

$$m_m\ddot{x_r} + c_m\dot{x_r} + k_m x_r = \alpha c_m\dot{d} + \alpha k_m d - \alpha F_f \quad (4)$$

EM of the slider is represented as:

$$m_s\ddot{x}_s = F_f - F_g \quad (5)$$

These equations are separately analyzed under two cases: stick and slip conditions.

(A) Stick condition

We assume that the condition of the stick is represented as,

$$\ddot{x_s} = \ddot{x_r}$$
$$\dot{x_s} = \dot{x_r} \quad (6)$$

$$x_s = x_r + x_{s0} \quad (7)$$

$$F_f \le \mu_0 F_N \quad (8)$$

From (4) and (5), by eliminating F_f, we obtained the following equation for the slider during the stick condition.

$$(m_m + \alpha m_s)\ddot{x}_s + c_m\dot{x_s} + k_m(x_s - x_{s0}) = \alpha c_m\dot{d} + \alpha k_m d - \alpha F_g \quad (9)$$

(B) Slip condition

During the slip condition, we approximate that the friction force becomes the constant kinetic friction force as $\mu_k F_N$, which is generated against the slip motion as below,

When $\dot{x}_R(t) - \dot{x}_s(t) > 0$
$$F_f = \mu_k F_N \tag{10}$$

When $\dot{x}_R(t) - \dot{x}_s(t) < 0$
$$F_f = -\mu_k F_N \tag{11}$$

Using (10) and (11), EM of the slider during the slip condition is represented as,

When $\dot{x}_R(t) - \dot{x}_s(t) > 0$
$$m_s \ddot{x}_s = \mu_k F_N - F_g \tag{12}$$

When $\dot{x}_R(t) - \dot{x}_s(t) < 0$
$$m_s \ddot{x}_s = -\mu_k F_N - F_g \tag{13}$$

3.3 Approximation as uniformly accelerated motion

For simplification, we approximate the motion of the slider as uniformly accelerated with the stick condition as,

$$\ddot{x}_s(t) = \ddot{x}_r(t) = a_s = const. \tag{14}$$

$$|a_s| \leq \frac{\mu_0 F_N}{m_s} \tag{15}$$

Here, we define an initial condition as below,

$$x_s(0) = x_{s0} = 0 \tag{16}$$

$$\dot{x_s}(0) = 0 \tag{17}$$

From (14), (15), (16), and (17), the velocity and displacement are calculated as,

$$\dot{x_s}(t) = a_s t \tag{18}$$

$$x_s(t) = \frac{1}{2} a_s t^2 \tag{19}$$

Maximum displacement during the 1 stroke motion under the stick condition is equal to the maximum displacement of the rod as,

$$x_s(T) = A_r = \frac{1}{2} a_s T^2 \tag{20}$$

The period of the stick motion is represented as,

$$T = \sqrt{\frac{2A_r}{a_s}} \tag{21}$$

If the velocity is approximately zero during the slip motion and the displacement is approximately constant, the approximated constant velocity is represented as,

$$\tilde{v}_s = \frac{1}{T}\int_0^T \dot{x_s}(t)dt = \frac{a_s}{T}\int_0^T t dt = \frac{a_s T}{2} = \sqrt{\frac{a_s A_r}{2}} \tag{22}$$

Approximated displacement of the slider is represented as,

$$\tilde{x}_s = \tilde{v}_s t \tag{23}$$

The maximum acceleration of a_{s_m} with upward motion is obtained from (5) and (8) as given by,

When upward motion,

$$a_{s\_m\_u} = \frac{\mu_0 F_N - F_g}{m_s} \tag{24}$$

When downward motion,

$$a_{s\_m\_d} = \frac{-\mu_0 F_N - F_g}{m_s} \tag{25}$$

From (21),

$$a_s = \frac{2A_r}{T^2} \tag{26}$$

Substituting (28) into (22),

$$\tilde{v}_s = \frac{A_r}{T} \tag{27}$$

From (23),

$$\tilde{x}_s = \frac{A_r}{T} t \tag{28}$$

When upward motion,

$$\tilde{v}_{s\_u} = \frac{A_r}{T} \leq \sqrt{\frac{A_r a_{s\_m\_u}}{2}} \tag{29}$$

$$\tilde{x}_{s\_u} = \frac{A_r}{T} t \leq \sqrt{\frac{A_r a_{s\_m\_u}}{2}}\, t \tag{30}$$

We use (28) as theoretical displacement for evaluating experimental motions.

3.4 Experiments

To investigate the basic performance of the actuator, we measured the displacement under several conditions. We used an optical linear encoder (TA-200, technohands) for measuring the displacement, which has a measurement resolution of 0.1 [μm] and the maximum sampling frequency is 2.8 [MHz].

In this experiment, theoretical displacement is obtained from (28). with approximations that the slider performs uniformly acc elerated motion, the slip time is zero, and there is no return dis placement. Index parameter values are shown in table 2.

Firstly, 150 [$V_{p\text{-}p}$] sinusoidal voltage with a frequency 1 [Hz] was applied for 10 cycles to evaluate the displacement of per one cycle under quasi static condition, and an average amplitude of displacement was measured. As a result, the average displacement value of 11.6 [μ m] was obtained, which is used as the reference amplitude as $\boldsymbol{A_{re}}$.

Secondly, two type waves, a sawtooth wave, and an inverse sawtooth wave, were applied for 10 cycles each at a driving frequency of 10 [Hz], and the amount of movement in both directions was measured. This experiment was conducted on a horizontal plane, for eliminating the gravity force of slider of $\boldsymbol{F_g}$. The average movement per cycle was calculated and compared with the theoretical value. The results are shown in Figure 4 and Table 3.

In results, the reduction ratio of the reference displacement of $\boldsymbol{A_{re}}$ to the theoretical value of $\boldsymbol{A_r}$ is 21.7 [%]. The reduction rates were 41.9 [%] and 23.5 [%] for the sawtooth and inverse sawtooth shaped input voltage against $\boldsymbol{A_r}$, respectively. Almost twice of the difference of the reduction rate, were indicating there is directional specificity. We thought that be caused by the difference in the mechanical response of the rod during rapid deformation due to the difference in the direction of expansion and contraction of the piezoelectric actuator. We also observed that the non-negligible oscillations occurred around every slip motions. Those vibration should be dumped for precise manipulation.

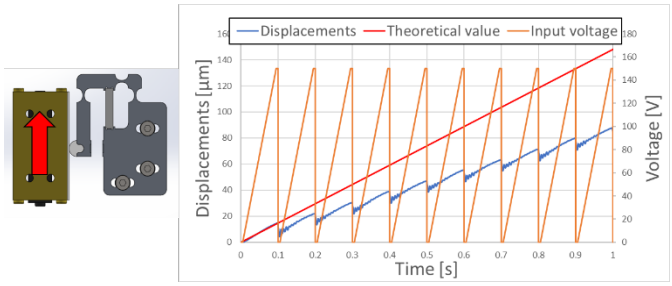

(a) Sawtooth wave

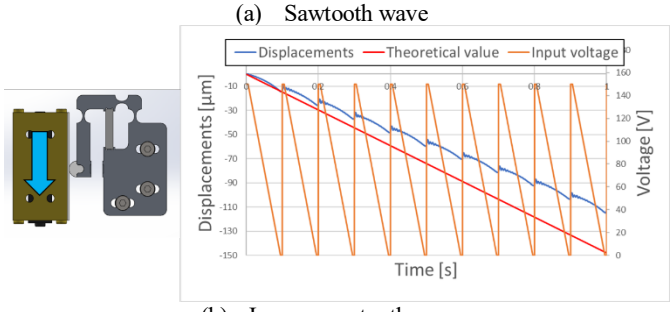

(b) Inverse sawtooth wave

Fig. 4 Plots of displacements vs. time on a horizontal plane for F_g=0

Table 2 Parameters of actuator

Parameter	l [mm]	L [mm]	x_m [μm]	A_r [μm]
Value	6.75	13.5	7.4	14.8

Table 3 Comparison of amplitude displacements among theoretical, experimental, and reference values.

	Avg. movement [μm]	Reduction rate from theoretical value [%]
Theoretical value (A_r)	14.8	
Reference value (A_{re})	11.6	21.7
Sawtooth wave	8.6	41.9
Inverse sawtooth wave	11.3	23.7

3.4 Configuration of the manipulator

As shown in fig. 5, we fabricated 2DoF manipulator using the two stick-slip actuators. The size is 47 [mm]×62 [mm]×48 [mm] and the mass is 55.3 [g], that is within the target in section 1. The manipulator consists of dual sets of actuators and sliders, one of for driving the Z-axis and the other for driving tweezers. The Z-axis travel range and the distance between two tips of the tweezers depend on the movable distance of the slider. In this case, the same slider is used, so the movable length is 13 [mm]. In addition, Z-axis driven linear slider is equipped with a liner scale and an optical encoder to measure the vertical displacement.

Next, we measured the drive of the manipulator at each drive frequency using this encoder system. The measurement results are shown in Fig. 6. As a result, the maximum speed was 8.9 [mm/s], and directional specificity was observed in the vertical direction due to the directional specificity and a gravity force of F_g.

6. Conclusion and future prospect

This paper described the construction of a compact piezoelectric stick-slip manipulator. The manipulator, had the size of 47 [mm]×62 [mm]×48 [mm] and the mass of 55.3 [g], and the maximum speed of

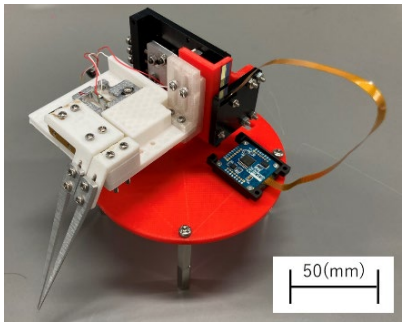

Fig.5 2DoF manipulator using two stick-slip actuators

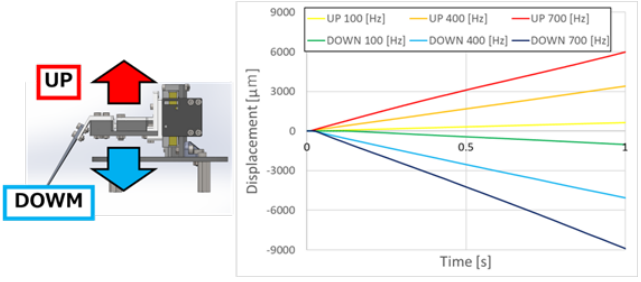

Fig. 6 Plots of Z-axis displacement of the manipulator vs. time

Z-axis was 8.9 [mm/s]. Additionally, we defined a mechanical model of the actuator, to analyze the dynamic characteristics. We measured the displacements in several conditions.

As a result, this manipulator has a directional specificity, and non-negligible oscillation caused by the slip motion. We consider that we need to reduce the oscillation by feedforward and feedback controls, for precise and delicate manipulation.

We plan to attach it on a holonomic mobile robot and implement manipulation. Moreover, automation of manipulation using image recognition technology based on machine learning is also one of the important subject to realize the flexible and precise mobile manipulator.

ACKNOWLEDGEMEN

Parts of this work were supported by the Tsugawa Foundation in 2022, Amano Institute of Technology in 2023, and Takahashi Industrial and Economic Research Foundation in 2023.

REFERENCES

1. J.Kim, An. Banks et al., “Miniaturized Flexible Electronic S ystems with Wireless Power and Near-Field Communication Capabilities”, Adv. Funct. Mater., 25, 4761–4767, 2015
2. S. H. Zheng, X. Y. Shi, P. Das, Z.-S. Wu, X. H. Bao, “The Road Towards Planar Microbatteries and Micro Supercapacitors: Fr om 2D to 3D Device Geometries”, Adv. Mater. 31, 1900583, 2019.
3. J.Cecil, M. B. Bharathi Raj Kumar, Yajun Lu, Vinod Basalla li, “A review of micro-devices assembly techniques and tech nology”, Int J Adv Manuf Technol, 83:1569–1581, 2016.

4. Mokrane Boundaoud, Stephane Regnier, “An Overview on G ripping Force Measurement at the Micro and Nano-scales Us ing Two-fingered Microrobotic Systems”, Int Adv Robot Sys t, 11:45, 2014.
5. Fuchiwaki, O. Ito, A. Misaki, D. Aoyama, H. “Multi-axial micromanipulation organized by versatile micro robots and micro tweezers” In Proceedings of the 2008 IEEE International Conference on Robotics and Automation, Pasadena, CA, USA, pp. 893–898, 2008.
6. Tanabe. K, Shiota. M, Kusui. E, Iida. Y, Kusama. H, Kinoshita. R, Tsukui. Y, Minegishi. R, Sunohara. Y, Fuchiwaki. O,” Precise Position Control of Holonomic Inchworm Robot Using Four Optical Encoders”, Micromachines 14, 375, 2023.
7. Allen. H, William. C, Cregg. C, Brian. M, Annjoe. W. F, R on. P, Joseph. L, “Diamagnetically levitated Milli-robots for heterogeneous 3D assembly”, Journal of Micro-Bio Robotics, 14:1–16, 2018.
8. Tristan Abondance, Kaushik Jayaram, Noah T. Jafferis, Jennifer Shum, Robert J. Wood, “Piezoelectric grippers for mobile micromanipulation”, IEEE Robotics and Automation Letters (RAL) paper presented at the 2020 IEEE/RSJ International Conference on Intelligent Robots and Systems (IROS) October 25-29, Las Vegas, NV, USA, 2020
9. Shijing Zhang, Yingxiang Liu, Jie Deng, Xiang Gao, Jing Li, Weiyi Wang, Mingxin Xun, Xuefeng Ma, Qingbing Chang, Junkao Liu, Weishan Chen, Jie Zhao, “Piezo robotic hand for motion manipulation from micro to macro”, Nature Communications, 14:500, 2023.
10. Alireza Fath, Tian Xia, Wei Li, “Recent Advances in the Application of Piezoelectric Materials in Microrobotic Systems”, Micromachines, 13, 1422, 2022.
11. Ravi K. Jain, Somajoyti Majumder, Bhaskar Ghosh, Surajit Saha, “Design and manufacturing of mobile micro manipulation system with a compliant piezoelectric actuator based micro gripper”, Journal of Manufacturing Systems, 35, 76-91, 2015.